Porous Liquid Phases for Indented Colloids with Depletion Interactions

Douglas J. Ashton, Robert L. Jack, and Nigel B. Wilding
Department of Physics, University of Bath, Bath BA2 7AY, United Kingdom
(Received 30 January 2015; revised manuscript received 28 April 2015; published 12 June 2015)

We study indented spherical colloids, interacting via depletion forces. These systems exhibit liquid-vapor phase transitions whose properties are determined by a combination of strong "lock-and-key" bonds and weaker nonspecific interactions. As the propensity for lock-and-key binding increases, the critical point moves to significantly lower density, and the coexisting phases change their structure. In particular, the liquid phase is porous, exhibiting large percolating voids. The properties of this system depend strongly on the topological structure of an underlying bond network: we comment on the implications of this fact for the assembly of equilibrium states with controlled porous structures.

DOI: 10.1103/PhysRevLett.114.237801 PACS numbers: 64.75.Xc, 61.20.Ja

In colloidal systems, a wide range of structures can be self-assembled from a simple palette of components and interactions [1]. For example, anisotropic forces between particles can stabilize colloidal micelles or exotic crystals [2–9], which could form the basis of future materials and devices. Anisotropic attractions can be achieved experimentally via chemical patches [2,6,10–12], or through a combination of particle shape and depletion forces [4,5,13–16]. Depletion forces arise when colloids are dispersed in a solution of much smaller depletant particles, which induce an attractive interaction [17], whose properties can be tuned via the size and number density of the depletant. These forces are relevant for the assembly of indented ("lock-and-key," LK) colloidal particles, which have recently been synthesized in experiments [4,18]. Here, we use Monte Carlo simulations to investigate the assembly of such particles [4,18–23]. Starting from simulations of indented colloids in the presence of an ideal depletant [24], we define an effective potential which captures quantitatively the depletion interaction. This enables efficient simulation, and accurate characterization of the liquid-vapor phase transitions that occur in this system. When the depletant particles are small in size compared to the colloids, the resulting liquid and vapor phases have unusual properties. In particular, the critical point for the phase transition occurs at a rather low density, and the liquid phases have a complex structure that includes a network of branched chains and large voids. Indeed, we find that the liquid phase is porous on a length scale comparable with the colloids.

An indented colloidal particle is modeled as a sphere of diameter σ, from which we cut away its intersection with a second sphere of the same diameter [21,22]. The distance between the sphere centers is taken as $d_c = 0.6\sigma$, so the depth of the indentation (measured from the lip) is 0.2σ, comparable with experimentally realizable particles [4]. The orientation of particle i is specified by a unit vector $\boldsymbol{n}_i$ that points outwards through the center of the indentation. The hard particle interactions between these particles are treated exactly in our model, but we parameterize the depletion interaction between the colloids through an effective potential, illustrated in Fig. 1. Specifically, when two colloids approach one another in the back-to-back (BB) configuration, they feel a square-well interaction potential of depth $\varepsilon_{\mathrm{BB}}$ and range r_{BB}. When they approach in the lock-key configuration, the interaction range is r_{LK}, and the effective potential also depends on the angle ϕ between the particle directors. For perfect lock-key binding, the depth of the potential well is $\varepsilon_{\mathrm{LK}}$. We fix the unit of energy by setting $\beta = 1/(k_B T) = 1$. The interaction ranges are fixed throughout this work according to $(r_{\mathrm{LK}} - d_c) = (r_{\mathrm{BB}} - \sigma) = 0.1\sigma$, comparable with the size of the depletant particles. (As for spherical particles [25], the behavior depends weakly on these interaction ranges, if the interaction strengths are adjusted so that the

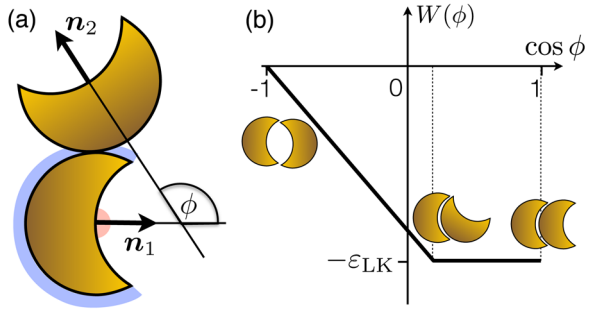

FIG. 1 (color online). Illustration of the effective potential between indented colloids. (a) The interaction depends on the vector $\boldsymbol{r}_{12}$ between the colloids, and their orientations $\boldsymbol{n}_{1,2}$. We define two angles θ_R and ϕ by $\cos\theta_R = \max(\boldsymbol{n}_1 \cdot \boldsymbol{r}_{12}, -\boldsymbol{n}_2 \cdot \boldsymbol{r}_{12})$ and $\cos\phi = \boldsymbol{n}_1 \cdot \boldsymbol{n}_2$. Particles can bind in a lock-key configuration (small θ_R) or a back-to-back configuration (large θ_R), as indicated by the two shaded areas. (b) In the lock-key orientation, the interaction depends on the angle ϕ through the function $W(\phi)$, the form of which is motivated by studies of the exact depletion potential [28].

binding free energies or second virial coefficients for pair interactions are held constant, and the ranges are small compared to σ.) To obtain the interaction strengths ε_{LK} and ε_{BB} as a function of depletant parameters, we used the geometric cluster algorithm (GCA) [26,27] to simulate systems of two colloidal particles interacting with a depletant of penetrable spheres [24]. The size ratio between colloids and depletant particles is q (the depletant diameter is $q\sigma$), and the reservoir volume fraction of the depletant is η_s. (That is, the chemical potential of the depletant is that of a system of pure depletant particles at volume fraction η_s.) Full details of the effective potential and the parameterization of $(\varepsilon_{LK}, \varepsilon_{BB})$ are given in the Supplemental Material [28].

We employed grand canonical Monte Carlo (GCMC) simulation to study the phase behavior [32,33] of the colloids, interacting through the effective potential, in cubic boxes of sizes between $(12\sigma)^3$ and $(20\sigma)^3$. Smaller boxes sufficed for large q, where the size of bound clusters is typically small; bigger boxes were needed to accommodate the larger clusters that form at small q. Our GCMC method uses the usual particle updates (insertions, deletions, displacements and rotations), combined with biased insertions and deletions, which attempt to add (or remove) a colloid in a lock-key bound state, subject to satisfying detailed balance. This innovation, (described further in the Supplemental Material [28]), increases the efficiency of the simulation by up to 4 orders of magnitude.

Figure 2(a) summarizes the phase behavior of the indented colloids. The state point of the system is specified by three parameters $(\rho, \varepsilon_{LK}, \varepsilon_{BB})$ where ρ is the number density of colloids. The solid line in Fig. 2(a) indicates values of $(\varepsilon_{LK}, \varepsilon_{BB})$ for which a liquid-vapor critical point exists, at some critical density ρ^c. For values of $(\varepsilon_{LK}, \varepsilon_{BB})$ above this line, there exist values of the density for which liquid-vapor phase coexistence occurs: see for example Figs. 2(b) and 2(c). The structure of these phases is discussed further below. Dotted lines in Fig. 2(a) show how the parameters of the effective model are related to depletant parameters (q, η_s): for smaller q, lock-key binding is more favorable than back-to-back binding. Increasing η_s at constant q leads to an increase in both ε_{LK} and ε_{BB}, along the dotted lines. To assess the accuracy of the effective potential, we used the GCA within a restricted Gibbs ensemble [34] to locate the critical point in a system of indented colloids with an explicit depletant, for $q = 0.2$. We find that the critical parameters lie within 10% of the results obtained with the effective potential. This confirms the effectiveness of our coarse-graining scheme, which being based on virial coefficient matching is expected to hold for more general colloid and depletant interactions than the idealized ones considered here. However, with an explicit depletant, it is not generally possible to investigate the structure of liquid and vapor phases, nor the behavior for smaller q, due to the computational cost required. Hence our use of the effective potential in this work.

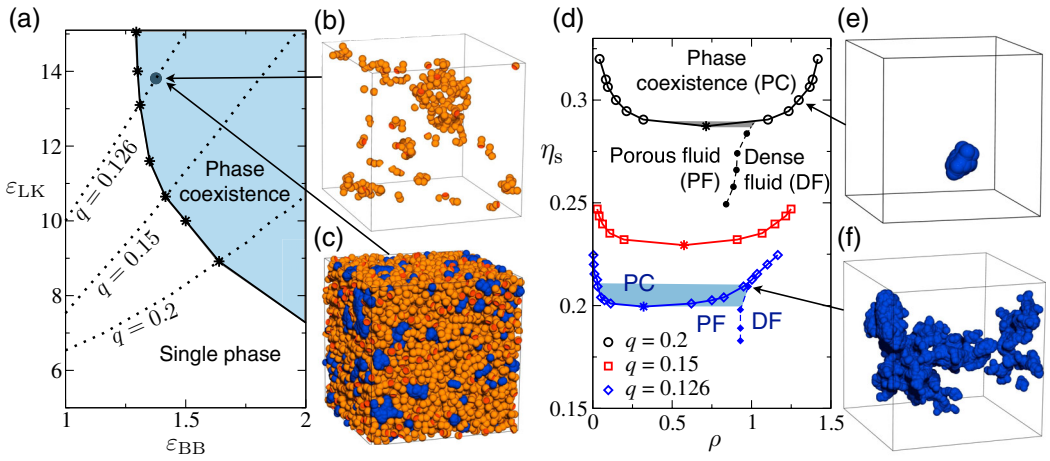

FIG. 2 (color online). (a) Summary of phase behavior, as a function of $\varepsilon_{LK}, \varepsilon_{BB}$. In the shaded region, coexistence of liquid and vapor phases can occur, for suitable colloid densities ρ. The stars indicate the positions of critical points. The dotted lines show how the effective interaction strengths $(\varepsilon_{LK}, \varepsilon_{BB})$ depend on the depletant size ratio q (the depletant volume fraction η_s varies along these lines). (b),(c) Representative configurations from the coexisting liquid and vapor phases at the indicated state point, which corresponds to $\eta_s = 1.05\eta_s^c$. For the liquid state, the void space is colored blue, to emphasize the porous structure. (d) Binodal curves showing the densities of coexisting liquid and vapor phases as a function of depletant parameters q, η_s and (total) colloid density ρ. Stars mark critical points. For $q = 0.126$ and $q = 0.2$, the dashed lines show the densities at which the void spaces percolate the system, as discussed in the main text. For the same values of q, shaded regions indicate regions where porous liquid states are found, either as pure phases or in coexistence with colloidal vapor: for $q = 0.2$ this is a very small region around criticality but for $q = 0.126$, there exists a well-defined porous state, away from the critical point. (e),(f) Visualizations of the largest void spaces from representative configurations at the indicated state points, both of which correspond to $\eta_s = 1.05\eta_s^c$.

The binodal curves associated with liquid-vapor phase coexistence are shown in Fig. 2(d), as a function of the depletant volume fraction η_s, for three values of q. As the depletant particles get smaller (decreasing q at fixed η_s), the attractive forces between colloids get stronger, so phase separation occurs for smaller values of η_s. However, the most striking effect in Fig. 2(d) is the strong decrease (by more than a factor of 2) in the critical density of the colloids ρ^c. The origin of this effect is the very strong lock-key binding that occurs when q is small which leads to chain formation. Similar properties have also been found in model polymer liquids [35–37] and in the empty liquids that occur in patchy-particle models [38–43]. In our case, however, the emergence of chains and their condensation into a liquid occurs in a system which is not inherently patchy.

Figures 2(b) and 2(c) illustrate the unusual structures of the coexisting phases for $q = 0.126$, corresponding to strong lock-key binding. There are large void spaces within the liquid: we identify these by inserting spherical "ghost particles" of size σ_g into the system, wherever this is possible without overlapping an existing colloid (ghost particles may overlap with each other). We take $\sigma_g = \sigma$ except where otherwise stated, in which case the ghost particles are the same size as the colloids. The ghost particles, shown in Fig. 2(c), highlight the existence of the voids. At this state point, the depletant volume fraction is 5% greater than its critical value η_s^c, so the system is significantly outside the critical regime: these voids are not associated with critical fluctuations, but are intrinsic to the liquid states that occur for small q.

Figures 2(e) and 2(f) show the largest voids in two single-phase liquid configurations, at $q = 0.2$ and $q = 0.126$. To ensure that the configurations are directly comparable, they are both sampled at phase coexistence, with depletant volume fraction $\eta_s = 1.05\eta_s^c$. For the larger depletant ($q = 0.2$), all voids in the system are relatively small, and the state is similar to a conventional colloidal liquid. For the smaller depletant ($q = 0.126$), there is a single large void which spans the entire system [Fig. 2(f)], so we expect that a test particle of a size comparable with a colloid can travel freely through the liquid: the state is porous on this scale.

The ghost particles allow this effect to be analyzed quantitatively. Figure 3 shows the fraction f_{void} of the system volume that is accessible to ghost particles of varying diameters. For $\sigma_g = \sigma$, this fraction changes by more than 2 orders of magnitude, as q is decreased from 0.2 to 0.126. To provide a clear distinction between the porous states at small q and the more conventional colloidal liquids at larger q, we analyzed the (η_s-dependent) colloid densities ρ^{vp} for which the ghost particles percolate the system. Dashed lines in Fig. 2(c) indicate the boundaries between percolating and nonpercolating void spaces, for $q = 0.126$ and $q = 0.2$. The lines extend through the supercritical fluid ($\eta_s < \eta_s^c$) and into the liquid ($\eta_s > \eta_s^c$). We propose

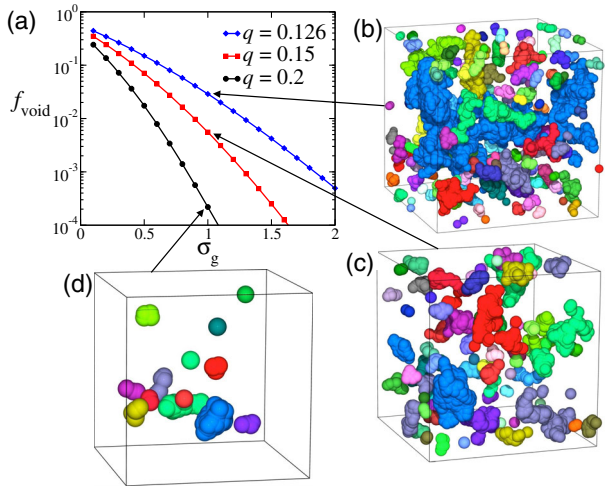

FIG. 3 (color online). (a) Fraction f_{void} of the system volume that is accessible to ghost particles of size σ_g, for liquid states at phase coexistence, with $\eta = 1.05\eta^c$, at various q. (b),(c),(d) Illustrations of the void spaces for liquid configurations for $q = (0.126, 0.15, 0.2)$, illustrating the increasing size and number of the voids as the liquid becomes more porous. Each connected void space is rendered in a different color, to emphasize the increasing connectedness of these spaces as q decreases.

that a *porous liquid* be defined as a state with $\eta > \eta_s^c$ for which the void space percolates, $\rho < \rho^{\text{vp}}$. We expect that some empty liquids [38,39,42] will also fall into this class. Shaded regions in Fig. 2(d) indicate regions where porous liquid states are found, either as pure phases or in coexistence with colloidal vapor. Clearly the single-phase porous liquid can exist only in a density range of width $\Delta\rho = \rho^{\text{vp}} - \rho^c$. For $q = 0.2$, one has $\Delta\rho \approx 0.3$ so porous liquids exist only very close to criticality. However, for $q = 0.126$ one has $\Delta\rho \approx 0.7$, so there is a significant density window in which porous liquids can be found. We expect this window to expand further at smaller q, indicating that small depletant particles would be most appropriate in experimental searches for such states.

The unusual structure of these porous liquid states originates from a hierarchy of energy scales—the system supports strong lock-key bonds, and weaker back-to-back binding. To illustrate this effect, imagine that the colloids form linear chains, connected by strong lock-key bonds [21]. For large ε_{LK}, almost all of the available lock sites are participating in binding—the weaker back-to-back binding then provides both interchain and intrachain interactions, which can cause the chains to aggregate or collapse, as happens in solutions of polymers [35–37,44]. However, chains of colloids linked by depletion forces are in fact akin to living polymers [45], in that they are continuously breaking and re-forming in the equilibrium state. One can associate the liquid state with an aggregated state of many polymers, while the unusual vapor phase contains polymeric chains that tend to collapse into compact states

[recall Fig. 2(b)]. In fact, Fig. 2(d) closely resembles the behavior of polymers in solution, interacting via a relatively weak nonspecific attraction [35–37]. As the polymer length increases in that system, the critical point moves to lower polymer density and weaker nonspecific interactions. The unusual liquid structure also affects critical properties (particularly field-mixing effects), as discussed in the Supplemental Material [28].

This analogy with polymers leads to a prediction for the colloidal system: in the limit of long polymers, one expects the liquid-vapor critical point to occur at the Θ temperature of the polymer [35–37], where the chain statistics are those of a simple random walk. This requires a weak nonspecific attraction, to overcome the excluded volume interactions that cause the polymer to swell. For the colloidal system, the long-polymer limit corresponds to $\varepsilon_{\mathrm{LK}} \to \infty$, in which case one would expect the liquid-vapor critical point to occur when the nonspecific (back-to-back) interaction $\varepsilon_{\mathrm{BB}}$ balances the excluded volume swelling effect [46]. This implies that the line of critical points in Fig. 2(a) should tend to a nonzero value of $\varepsilon_{\mathrm{BB}}$, as $\varepsilon_{\mathrm{LK}} \to \infty$, consistent with our results.

However, while this analogy between chains of indented colloids and linear living polymers is appealing, it misses an important feature of the colloidal system. For the particle shape considered here, these colloids readily form *branched* chains. In simple patchy-particle models (with a single type of attractive patch), the presence of branching is sufficient to drive a liquid-vapor phase transition [38–42,46,47], but this is not the case for lock-and-key colloids. The reason is the directed nature of the lock-key bond. In Fig. 4, we illustrate different local structures in these systems, and the construction of a bond network. Lock-key bonds are indicated by arrows that point from the lock particle to the key. In this representation, the crucial feature is that a particle may have several inward bonds, but at most one outward bond. It follows that a cluster of particles connected by lock-key bonds may contain at most one loop, as illustrated in Fig. 4(b). In patchy particle models, directed bonds can be realized by introducing more than one kind of patch, which can lead to similar phase behavior to that reported here [46,47]. This effect can be illustrated using Wertheim's theory of associating fluids [21,38,39,48], as discussed in the Supplemental Material [28].

These results illustrate the subtle role of the bonding topology in hierarchical fluids. Loops are essential for condensation—they may arise either from undirected branching [38,39] or from nonspecific interactions [35–37]. Yet another point of reference is provided by dipolar fluids [49,50] and other related systems [51], where formation of ring (or loop) structures acts to *suppress* condensation, due to the absence of nonspecific interactions between closed rings, and the low probability of branching. Thus, while the formation of colloidal polymers can occur for several kinds of particle, the energy scales associated with liquid-vapor phase separation can be quite different, as can the properties of the coexisting phases.

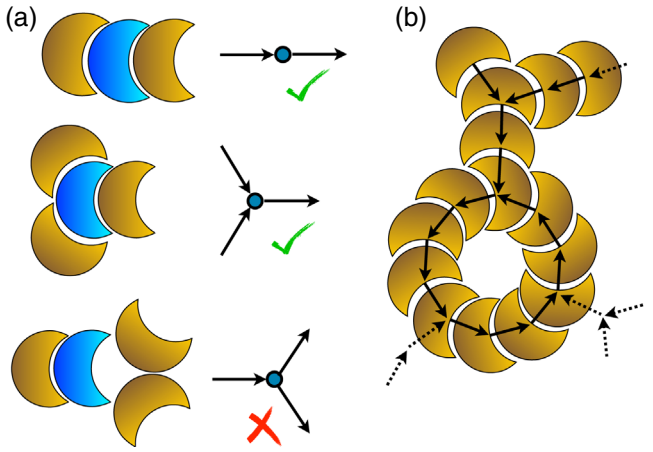

FIG. 4 (color online). (a) Network motifs for lock-key bonds. Circles indicate particles and arrows indicate lock-key bonds, directed from the lock to the key. The most important local environments are linear chains (one outward and one inward bond) and branching points (two inward and one outward bond). The converse branching case (one inward and two outward bonds) is not possible, due to the particle shape. (b) Clusters of particles can be characterized by networks of arrows. Once a connected cluster of particles includes a single loop, it can grow further only by forming inward bonds (some possible locations for additional bonds are shown with dotted arrows). It follows that each connected cluster can include at most one loop.

In conclusion, indented colloids with depletion interactions support unusual liquid and vapor phases, which arise from a hierarchy of energy scales for lock-key and back-to-back binding. In particular, for small q, liquid phases of indented colloids are porous, characterized by large percolating voids. As shown in Figs. 2 and 3, the volumes associated with these voids can be tuned over several orders of magnitude by varying the properties of the depletant fluid. Indented colloids share some properties with empty liquids [38,39,42,47] and dipolar fluids [49–51]. These similarities indicate that porous liquids might be accessible in those systems too. However, the fine experimental control that can be achieved by manipulation of particle shape and depletant properties [17] makes indented colloids ideal for further experimental study in this direction, offering the potential for preparation of equilibrium gels [38,42,52] with controllable properties.

We are grateful to the EPRSC for support for D. J. A. and N. B. W. through Grant No. EP/I036192/1 and support for R. L. J. through Grant No. EP/I003797/1.

[1] S. Glotzer and M. Solomon, Nat. Mater. **6**, 557 (2007).
[2] Y. Wang, Y. Wang, D. R. Breed, V. N. Manoharan, L. Feng, A. D. Hollingsworth, M. Weck, and D. J. Pine, Nature (London) **491**, 51 (2012).

[3] N. B. Schade, M. C. Holmes-Cerfon, E. R. Chen, D. Aronzon, J. W. Collins, J. A. Fan, F. Capasso, and V. N. Manoharan, Phys. Rev. Lett. **110**, 148303 (2013).
[4] S. Sacanna, W. T. M. Irvine, P. M. Chaikin, and D. J. Pine, Nature (London) **464**, 575 (2010).
[5] L. Rossi, S. Sacanna, W. T. M. Irvine, P. M. Chaikin, D. J. Pine, and A. P. Philipse, Soft Matter **7**, 4139 (2011).
[6] Q. Chen, S. C. Bae, and S. Granick, Nature (London) **469**, 381 (2011).
[7] S. Sacanna, L. Rossi, and D. J. Pine, J. Am. Chem. Soc. **134**, 6112 (2012).
[8] N. K. Ahmed, G. van Anders, E. R. Chen, and S. C. Glotzer, arXiv:1501.03130.
[9] G. van Anders, D. Klotsa, N. K. Ahmed, M. Engel, and S. C. Glotzer, Proc. Natl. Acad. Sci. U.S.A. **111**, E4812 (2014).
[10] D. J. Kraft, J. Groenewold, and W. K. Kegel, Soft Matter **5**, 3823 (2009).
[11] D. J. Kraft, J. Hilhorst, M. A. P. Heinen, M. J. Hoogenraad, B. Luigjes, and W. K. Kegel, J. Phys. Chem. B **115**, 7175 (2011).
[12] M. E. Leunissen, R. Dreyfus, F. C. Cheong, D. G. Grier, R. Sha, N. C. Seeman, and P. M. Chaikin, Nat. Mater. **8**, 590 (2009).
[13] X. Xia and Y. Xia, Nano Lett. **12**, 6038 (2012).
[14] A. P. Gantapara, J. de Graaf, R. van Roij, and M. Dijkstra, Phys. Rev. Lett. **111**, 015501 (2013).
[15] S. Sacanna, D. J. Pine, and G.-R. Yi, Soft Matter **9**, 8096 (2013).
[16] M. Marechal, R. J. Kortschot, A. F. Demiroers, A. Imhof, and M. Dijkstra, Nano Lett. **10**, 1907 (2010).
[17] H. N. W. Lekkerkerker and R. Tuinier, *Colloids and the Depletion Interactions*, Lecture Notes in Physics Vol. 833 (Springer, Berlin/Heidelberg, 2011).
[18] S. Sacanna, W. T. M. Irvine, L. Rossi, and D. J. Pine, Soft Matter **7**, 1631 (2011).
[19] G. Odriozola, F. Jimenez-Angeles, and M. Lozada-Cassou, J. Chem. Phys. **129**, 111101 (2008).
[20] D. Ortiz, K. L. Kohlstedt, T. D. Nguyen, and S. C. Glotzer, Soft Matter **10**, 3541 (2014).
[21] D. J. Ashton, R. L. Jack, and N. B. Wilding, Soft Matter **9**, 9661 (2013).
[22] D. J. Ashton *et al.*, arXiv:1412.1596.
[23] P.-M. König, R. Roth, and S. Dietrich, Europhys. Lett. **84**, 68006 (2008).
[24] S. Asakura and F. Oosawa, J. Chem. Phys. **22**, 1255 (1954).
[25] M. G. Noro and D. Frenkel, J. Chem. Phys. **113**, 2941 (2000).
[26] C. Dress and W. Krauth, J. Phys. A **28**, L597 (1995).
[27] J. Liu and E. Luijten, Phys. Rev. Lett. **92**, 035504 (2004).
[28] See Supplemental Material at http://link.aps.org/supplemental/10.1103/PhysRevLett.114.237801 for details of our model parameterization, simulation methodology and theory concerning the effects of branching and non-specific interactions on phase behavior, which includes Refs. [29–31].
[29] C. Law, N. B. Wilding, and R. L. Jack (to be published).
[30] J. P. Hansen and I. R. McDonald, *Theory of Simple Liquids* (Academic, London, 2006).
[31] Y. C. Kim, M. E. Fisher, and G. Orkoulas, Phys. Rev. E **67**, 061506 (2003).
[32] N. B. Wilding, Phys. Rev. E **52**, 602 (1995).
[33] A. D. Bruce and N. B. Wilding, Phys. Rev. Lett. **68**, 193 (1992).
[34] D. Ashton, J. Liu, E. Luijten, and N. Wilding, J. Chem. Phys. **133**, 194102 (2010).
[35] N. B. Wilding, M. Muller, and K. Binder, J. Chem. Phys. **105**, 802 (1996).
[36] H. Frauenkron and P. Grassberger, J. Chem. Phys. **107**, 9599 (1997).
[37] A. Z. Panagiotopoulos, V. Wong, and M. A. Floriano, Macromolecules **31**, 912 (1998).
[38] E. Bianchi, J. Largo, P. Tartaglia, E. Zaccarelli, and F. Sciortino, Phys. Rev. Lett. **97**, 168301 (2006).
[39] E. Bianchi, P. Tartaglia, E. Zaccarelli, and F. Sciortino, J. Chem. Phys. **128**, 144504 (2008).
[40] E. Bianchi, P. Tartaglia, E. La Nave, and F. Sciortino, J. Phys. Chem. B **111**, 11765 (2007).
[41] J. Russo, J. M. Tavares, P. I. C. Teixeira, M. M. T. da Gama, and F. Sciortino, J. Chem. Phys. **135**, 034501 (2011).
[42] B. Ruzicka, E. Zaccarelli, L. Zulian, R. Angelini, M. Sztucki, A. Moussaïd, T. Narayanan, and F. Sciortino, Nat. Mater. **10**, 56 (2011).
[43] S. Biffi, R. Cerbino, F. Bomboi, E. M. Paraboschi, R. Asselta, F. Sciortino, and T. Bellini, Proc. Natl. Acad. Sci. U.S.A. **110**, 15633 (2013).
[44] A. Y. Grosberg and A. R. Khokhlov, *Statistical Physics of Macromolecules* (American Institute of Physics, New York, 1994).
[45] K. M. Zheng and S. C. Greer, Macromolecules **25**, 6128 (1992).
[46] J. M. Tavares, P. I. C. Teixeira, and M. M. Telo da Gama, Phys. Rev. E **80**, 021506 (2009).
[47] J. M. Tavares, P. I. C. Teixeira, M. M. Telo da Gama, and F. Sciortino, J. Chem. Phys. **132**, 234502 (2010).
[48] M. S. Wertheim, J. Stat. Phys. **42**, 477 (1986).
[49] T. Tlusty and S. A. Safran, Science **290**, 1328 (2000).
[50] G. Ganzenmüller and P. J. Camp, J. Chem. Phys. **126**, 191104 (2007).
[51] L. Rovigatti, J. M. Tavares, and F. Sciortino, Phys. Rev. Lett. **111**, 168302 (2013).
[52] S. Roldán-Vargas, F. Smallenburg, W. Kob, and F. Sciortino, Sci. Rep. **3**, 2451 (2013).